Novel fluorescent CdTe quantum dot–thymine conjugate—synthesis, properties and possible application

2017 Nanotechnology 28 045701

(http://iopscience.iop.org/0957-4484/28/4/045701)

IOP Publishing Nanotechnology
Nanotechnology 28 (2017) 045701 (13pp) doi:10.1088/1361-6528/28/4/045701

Novel fluorescent CdTe quantum dot–thymine conjugate—synthesis, properties and possible application

Łucja Rodzik, Joanna Lewandowska-Łańcucka, Michał Szuwarzyński, Krzysztof Szczubiałka[1] and Maria Nowakowska[1]

Faculty of Chemistry, Jagiellonian University, Ingardena 3, 30-060 Kraków, Poland

E-mail: szczubia@chemia.uj.edu.pl and nowakows@chemia.uj.edu.pl

Received 6 September 2016, revised 12 October 2016
Accepted for publication 7 November 2016
Published 15 December 2016

Abstract

Novel, highly fluorescent cadmium telluride quantum dots conjugated with thymine and stabilized with thioglycolic acid were obtained and characterized. Successful formation of the conjugate was confirmed by elemental analysis, and UV–vis, fluorescence and Fourier transform infrared spectroscopies. Crystal structure and composition of the conjugates were characterized with xray diffraction and x-ray photoelectron spectroscopy. The size of the conjugates was 4–6 nm as demonstrated using atomic force microscopy and high resolution transmission electron microscopy imaging. The plasmon resonance fluorescence band at 540 nm on excitation at 351 nm was observed for these nanoparticles. The intensity of this band increased with the increase in the amount of conjugated thymine with no shift in its position. Based on the fluorescence measurements it was found that the CdTe–thymine conjugate interacted efficiently and selectively not only with adenine, a nucleobase complementary to thymine, but also with adenine-containing modified nucleosides, i.e., 5′-deoxy-5′-(methylthio)adenosine and 2′-O-methyladenosine, the urinary tumor markers which allow monitoring of the disease progression. To the best of our knowledge, as yet, there have been no studies presented in literature on that type of the interaction with CdTe–thymine conjugates. Therefore, the system presented can be considered as a working component of a selective adenine/adenosine biosensor with potential application in cancer diagnosis.

Keywords: CdTe, quantum dots, thymine, conjugate, photoluminescence

(Some figures may appear in colour only in the online journal)

1. Introduction

Quantum dots (QDs), known as nanoscale semiconductor crystals, have attracted considerable attention in recent years due to their unique electronic and optical properties [1–3]. QDs exhibit many attractive features, including large absorption coefficients, size-dependent, tunable, and efficient emission, as well as superior signal brightness [4–6]. The large surface area of QDs, the ease of their modification with different ligands [7, 8] and their resistance to photobleaching are important advantages of QDs over organic dyes [9, 10] and make them excellent fluorescent materials for use in various areas including nanotechnology, biomedicine or environmental monitoring [11–13]. In particular, biological research relies greatly on the availability of sensitive and selective fluorescent probes [14]. QDs seem to be a promising material for these applications, as found in recent studies. For example, QDs have been used as sensor materials for detecting small molecules [15], compounds with biochemical functions [16], ions [17] and toxic molecules [18]. Also, QDs could be used to monitor pH, temperature and oxygen level [19] and as a component of biosensors, which are small devices aimed at the detection of target analytes which are usually biomolecules such as proteins and nucleic acids [20].

[1] Authors to whom any correspondence should be addressed.

They use biological molecules to recognize the target and to translate its presence into electrical or optical mass sensitive signals allowing identification and the quantitative determination of the target molecules [21]. Thus, the biosensors provide a means of rapid, highly sensitive and real-time monitoring of biomolecules, including those of physiological interest [22].

Deoxyribonucleic acid (DNA) is a biomacromolecule serving as a carrier of genetic information used in the protein biosynthesis [23, 24]. Adenine and guanine (purines), thymine and cytosine (pyrimidines) are components of nucleotides, the building blocks of both DNA and RNA (in RNA thymine is replaced with uracil) [25]. The thymine–adenine and guanine–cytosine base pairing phenomenon is very important for maintaining the helical structure by DNA, in which two helical chains of nucleotides are held together by the hydrogen bonds, as demonstrated by Watson and Crick in 1953 [26]. Hydrogen bonds within the nucleobase pairs play a key role in the molecular theory behind the transcription and translation processes [27].

The abnormally high concentration of a nucleobase derivative suggests the deficiency of the immune system and may be indicative of various diseases. The increased level of these compounds in body fluids such as blood or urine is considered to be an important diagnostic of cancer, AIDS and the stage of these diseases while its steady and controlled decrease down to normal values may indicate success in therapy [28]. Therefore, the quantitative and qualitative analysis of these nucleobase derivatives is of great significance to clinical diagnosis.

The idea of the studies described in this paper was to obtain and characterize the QDs-nucleobase bioconjugates which could be used for the development of the novel fluorescent detection system of the derivatives of complementary nucleobases. In principle, the conjugation of the QDs with the appropriate ligand could allow the recognition of a target specifically bound by this ligand since the presence of the target in the direct vicinity of the QDs surface may change the properties of QDs luminescence [22]. For example, the interactions between a target molecule and the surface of QDs may influence the efficiency of the electron–hole recombination process leading to the change in the luminescence intensity [29, 30].

In the current study we have focused our attention on the preparation and characterization of the novel fluorescent materials based on thymine-conjugated cadmium telluride quantum dots (CdTe QDs–thymine). The role of thymine ligand was to interact selectively with adenine-containing biomarkers via the formation of the hydrogen bonds with the assumption that this interaction would affect the fluorescence of the QDs in a concentration-dependent manner.

To be useful in this biomedical application the QDs should form stable suspensions in water. This can be achieved by their functionalization with e.g., amphiphilic polymers [31], silica compounds [32], and thiols [33] such as glutathione, thioglycerol, or thioglycolic acid (TGA). Thiols are particularly often chosen for the functionalization of QDs [34]. The long-term stability of the QDs depends on the strength of bond between the thiol group and the QD surface. However, the moieties bound with thiol groups can be cleaved from the QD surface, causing the QDs to aggregate and precipitate from solution [35]. Thus, we have obtained stable suspensions of CdTe QDs modified with TGA using a facile one-pot method. We have selected TGA, since it allowed both stabilization of QDs in water and their further modification by providing free carboxyl groups which could react with thymine. Moreover, CdTe QDs stabilized with TGA are stable in both acidic and basic conditions and show increased photoluminescence efficiency [36]. The TGA-functionalized CdTe QDs can be dried and stored for several months as solid and redispersed in water when needed [34].

Subsequently, CdTe–thymine conjugates were successfully obtained in water by reacting water-soluble TGA-functionalized CdTe QDs with thymine. Successful formation of the conjugate was confirmed by elemental analysis, and UV–vis, fluorescence and Fourier transform infrared (FTIR) spectroscopies. The crystalline structure of the obtained material was characterized with x-ray diffraction (XRD). The composition of CdTe QDs and their thymine conjugate was also examined using x-ray photoelectron spectroscopy (XPS). The size of the materials developed was estimated using atomic force microscopy (AFM) and high resolution transmission electron microscopy (HRTEM) imaging. The interaction of the conjugate with optimized composition with different nucleobases and modified adenosine derivatives which are cancer markers was then studied using the fluorescence spectroscopy.

2. Materials and methods

2.1. Materials

Sodium borohydride ($NaBH_4$, Sigma Aldrich, 98%), tellurium powder (Sigma Aldrich, 99.999%), cadmium chloride ($CdCl_2 \cdot 5/2\ H_2O$, Sigma Aldrich), TGA (Sigma Aldrich, 98%), 2-propanol (Sigma Aldrich, 99.9%), thymine (TCI America, 98%), adenine (TCI America, 98%), guanine (TCI America, 98%), cytosine (TCI America, 98%), 5′-deoxy-5′-(methylthio) adenosine (MTA, Sigma Aldrich, 98%), 2′-O-methyladenosine (Sigma Aldrich, 98%) were used as received.

2.2. Apparatus

2.2.1. Elemental analysis. Elemental analysis was performed with a CHNS Vario Micro Cube Elemental Analyzer.

2.2.2. Spectrofluorometry. A F-2700 Hitachi spectrofluorimeter was used for fluorescence measurements. The excitation and emission slits were adjusted to 5 nm. Excitation wavelength was set at 351 nm.

2.2.3. Spectrophotometery. The electronic absorption spectra were measured with UV–vis spectrophotometer (Hitachi U-2900) using 1 cm quartz cuvettes.

2.2.4. Fourier transform infrared spectroscopy. FTIR spectroscopy was used to determine the effectiveness of

Table 1. The volumes and concentrations of reagents used in the synthesis of the conjugates.

CdTe:thymine molar ratio	V_{CdTe} (ml)	$V_{thymine}$(μl)	(Thymine) (μmol dm^{-3})
control	0.5	0	0
1:1	0.5	1.4	2.8
1:2	0.5	2.8	5.6
1:3	0.5	4.2	8.3
1:5	0.5	7.0	13.9
1:6	0.5	8.4	16.7
1:7	0.5	9.8	19.4

conjugation of thymine to CdTe QDs. The FTIR spectra were recorded using a Thermo Fisher Scientific Nicolet IR200 spectrometer. The samples for FTIR analysis were isolated from dispersion by drying in vacuum for 24 h.

2.2.5. Dynamic light scattering (DLS) and zeta potential measurements. A Malvern Nano ZS light-scattering apparatus (Malvern Instrument Ltd, Worcestershire, UK) was used for DLS and zeta potential measurements. The time-dependent autocorrelation function of the photocurrent was acquired every 10 s, with 15 acquisitions for each run. The sample of solutions was illuminated by a 633 nm laser, and the intensity of light scattered at an angle of 173° was measured by an avalanche photodiode. The z-averaged hydrodynamic mean diameter (dz), dispersity index (DI) and distribution profiles were calculated using the software provided by Malvern. The zeta potential was measured using the technique of laser Doppler velocimetry.

2.2.6. Transmission electron microscopy (TEM). TEM observations were carried out using FEI TECNAI TF20 X-TWIN high resolution transmission electron microscope. It is a 200 kV field emission gun microscope with a point resolution $\leqslant$0.25 nm. A 200 mesh copper grid coated with Formvar/carbon film (Pacific Grid-Tech) was dipped in the sample dispersion and left for about 20 min. The excess of the sample was blotted with a filter paper.

2.2.7. Atomic force microscopy. AFM images were obtained with Dimension Icon AFM (Bruker, Santa Barbara, CA) working in the PeakForce mode in the air at room temperature. Silicon tip on nitride cantilevers (Bruker) with nominal spring constant of 0.24 N m^{-1} and tip radius of 2 nm was used for the measurements.

2.2.8. X-ray diffraction. X'Pert PRO MPD diffractometer (PANalytical) with a Bragg–Brentano geometry was used for all XRD measurements. A copper x-ray sealed tube was used as the radiation source. Graphite monochromator was applied to select only Cu K_α (1.540598 Å–$K_{\alpha1}$ and $K_{\alpha2}$–1.544426 Å) radiation.

2.2.9. X-ray photoelectron spectroscopy. XPS analysis was carried out using a multifunctional ESCA instrument equipped with additional equipment produced by PREVAC. The vacuum chamber of the instrument was equipped with an 5-axial analytical precision manipulator, hemispherical charged particle analyzer XPS, UPS and AES (VG Scient R3000), two anticathodal x-ray tube Mg/Al (power Mg/Al 400/600 W), x-ray monochromator (three crystals) with the radiation source (a single Al anticathode, 600 W), pumping and measuring vacuum system (provided the vacuum base $<1 \times 10^{-8}$ mbar after 48 h annealing at 150 °C), the charge neutralizing gun (FS40-PS) on the surface of non-conducting samples (energy range 0–500 eV, electron current 1–500 μA), the ion gun to perform depth profiles (IS 40E-PS) and electron gun for the Auger spectroscopy (ES 40C-PS). For XPS experiment the QDs dispersions were dried in a vacuum for 24 h.

2.3. Preparation of stable suspensions of CdTe QDs

The CdTe QDs were prepared in the reaction between Cd^{2+} and NaHTe in the presence of TGA acting as the stabilizing agent using procedure described by Wei and coworkers [37] with slight modifications. Briefly, sodium borohydride (150 mg, 4.0 mmol) was reacted with tellurium powder (25.5 mg, 0.20 mmol) in water to produce NaHTe. This reaction was carried out under argon till the color of the solution changed to light pink. Cadmium chloride (90 mg, 0.49 mmol) was dissolved in 100 ml deionized water and 66.7 μl (0.96 mmol) of TGA was added to that solution under stirring. The pH value was adjusted to 11.2 by the addition of 10.0 mol l^{-1} NaOH solution dropwise. The resulting solution was degassed by bubbling nitrogen for 30 min and freshly prepared NaHTe was injected into it under vigorous stirring and the reaction was carried out under nitrogen at 95 °C for another 1 h. The solution changed from colorless to orange. After synthesis the CdTe QDs were purified by precipitation with 2-propanol. The obtained orange-colored powder was dried at room temperature in the vacuum.

2.4. Preparation of CdTe–thymine conjugates

To obtain CdTe–thymine conjugates the dispersion of purified CdTe QDs (1 mg ml^{-1}) in the PBS buffer (0.5 ml, 0.1 mol l^{-1}, pH = 7.5) and various volumes of thymine solution (1 mg ml^{-1}, 7.9 mmol l^{-1}) were mixed (see table 1). The resulting dispersions were diluted to the same volume (4 ml) with PBS buffer and mixed thoroughly. The mixtures were kept for 24 h in the dark in the ice-cooled bath before measuring the fluorescence spectra at room temperature.

3. Results and discussion

3.1. Synthesis and physicochemical characterization of CdTe QDs and CdTe–thymine conjugate

CdTe QDs were synthesized in water and stabilized with TGA. The process is schematically shown in figure 1(A).

TGA provides steric stabilization of CdTe QDs. It also passivates their surface by removing possible traps which

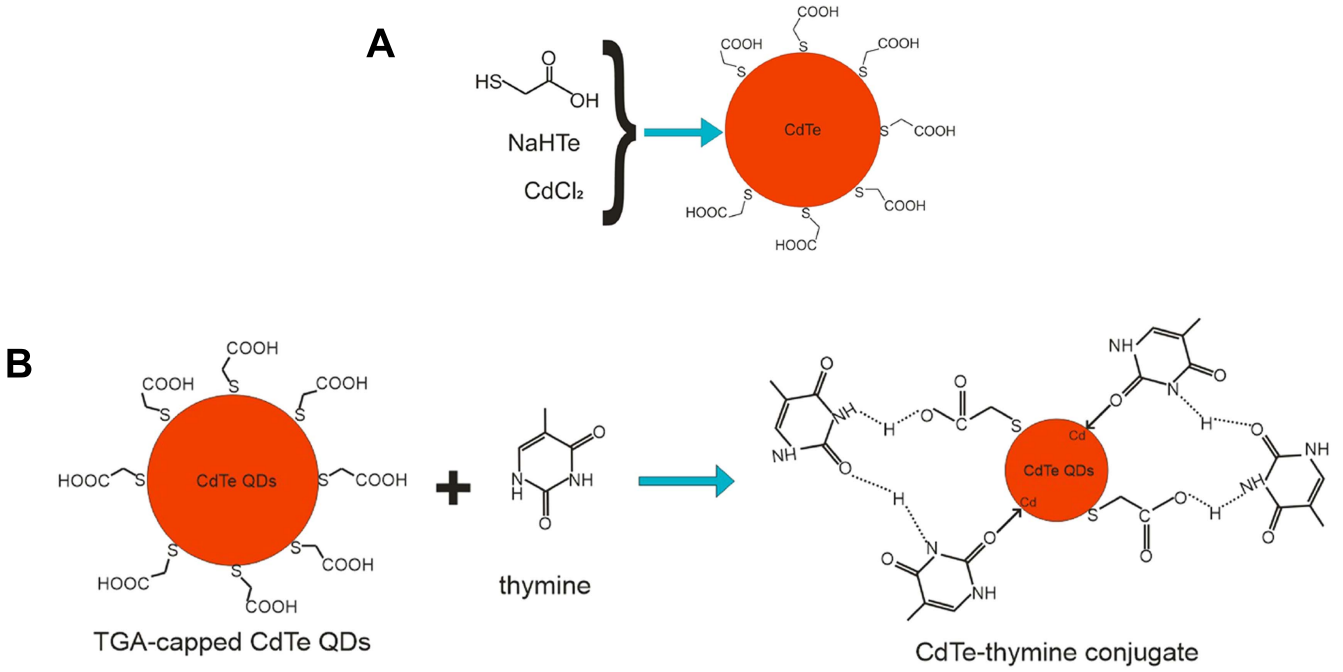

Figure 1. Synthesis of the TGA-capped CdTe QDs (A) and CdTe–thymine conjugates (B).

could lower the photoluminescence efficiency of the QDs and prevents the electron–hole recombination. Additionally, TGA controls the kinetics of particle growth and hinders their aggregation. This capping agent enables also covalent functionalization of the QDs and their interaction with other molecules through electrostatic forces and hydrogen bonding [38]. This interaction of QDs with their environment is crucial for the stability of their dispersions and photoluminescence properties [39]. The CdTe QDs obtained were characterized using various physicochemical techniques.

3.1.1. FTIR analyses. To confirm the covalent attachment of TGA to the QDs the FTIR spectra of TGA and CdTe QDs stabilized with TGA were compared (figure 2(A)). The absorption bands at 3440 cm^{-1} (OH stretching vibration), 2865 cm^{-1} (CH_2 symmetric stretching vibration), 1556 cm^{-1} (COO^- asymmetric stretching vibration), 1415 cm^{-1} (CH_2 scissoring vibration), 1369 cm^{-1} (COO^- symmetric stretching vibration), and 1145 cm^{-1} (CO stretching vibration) were observed for the TGA-capped CdTe QDs [40]. In addition, the absorption band at 2568 cm^{-1} which can be attributed to the S–H vibrations in TGA disappeared in TGA-capped CdTe QDs, confirming that TGA was covalently bound to the surface of the QDs which was accompanied by the disappearance of the S–H bonds and the formation of the S–Cd bonds. Considering that the asymmetric stretching vibration of the carbonyl group within the carboxylic group of TGA has shifted from 1711 to 1578 cm^{-1}, one can postulate that the carboxylic groups are deprotonated what provides additional electrostatic stabilization of the QDs. Based on these observations one can conclude that TGA should provide effective stabilization for CdTe QDs.

In the next step the CdTe–thymine conjugates with various number of thymine moieties bound to the QD surface were prepared. The process is schematically shown in figure 1(B). One of the most important parameters of this synthesis is pH of the reaction mixture. Feng *et al* [41] have recently shown that in order to prepare stable conjugates of CdTe QDs with guanine the pH value of the aqueous dispersion should be adjusted to 7.49 to maximize the efficiency of the formation of the hydrogen bonds between $–NH_2$ groups of guanine and –COOH groups of TGA present at the surface of QDs as well as to enable coordination of Cd^{2+} ions by the lone pair electrons of the oxygen atom of guanine. Taking into account these findings and the pKa value for thymine (equation (1)) we carried out the synthesis of CdTe–thymine conjugate in the PBS buffer (pH = 7.5) at constant ionic strength (I = 0.01 M).

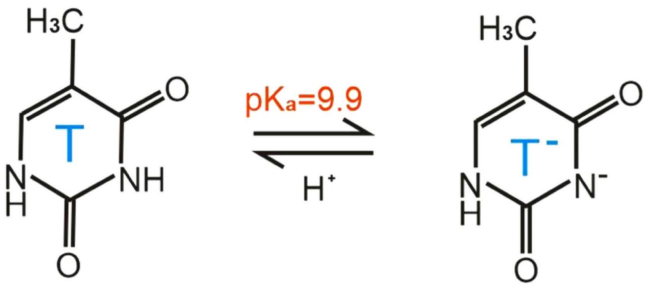

(1)

The conjugate formation was confirmed by elemental analysis and FTIR measurements. The results of elemental analysis for CdTe QDs and CdTe–thymine 1:6 conjugate are presented in table 2. The presence of sulfur in CdTe QDs provides an evidence for the stabilization of CdTe QDs with TGA while the presence of nitrogen in CdTe–thymine particles confirmed conjugation of CdTe QDs with thymine.

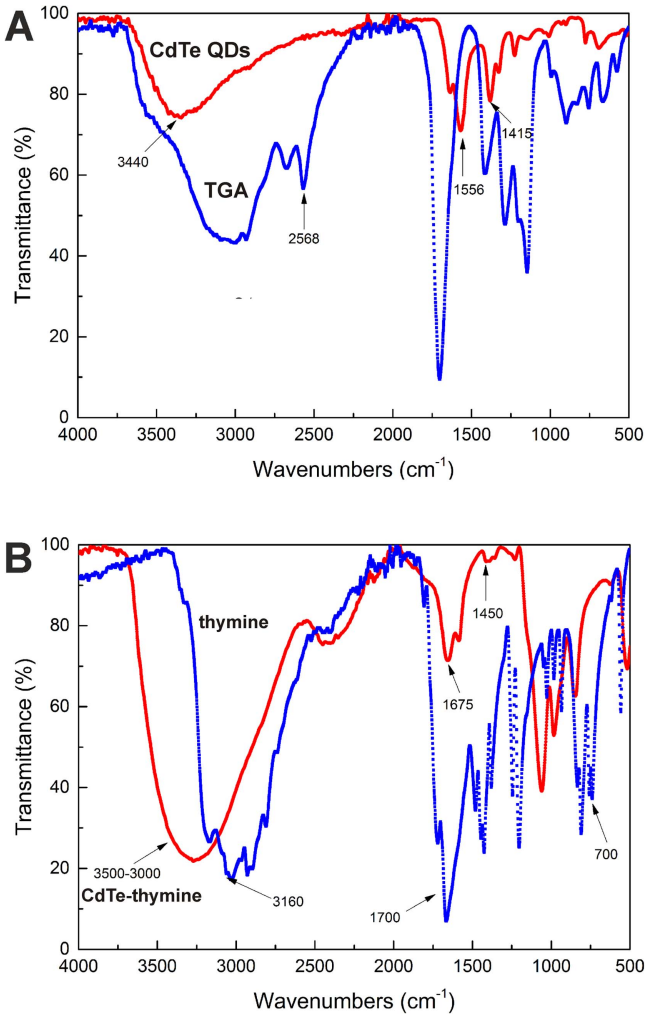

Figure 2. FTIR spectra of TGA and TGA-capped CdTe QDs (A) and FTIR spectra of thymine and the CdTe–thymine conjugate (B).

Figure 2(B) presents the FTIR spectra of thymine and CdTe–thymine conjugates. The absorption bands at 3185 and 3160 cm^{-1} of thymine are attributed to the stretching vibration of N–H groups while a band at 1700 cm^{-1} is characteristic of C=O vibration. The stretching modes of pyrimidine ring are the combinations of the stretching of the C–N, C=N, C–C and C=C bonds of the ring. The bands at 1445, 1290, 1240, 1030 and 700 cm^{-1} were assigned to the ring stretching modes [42]. Analysis of the spectrum of CdTe–thymine conjugate indicated that the absorption band present in the range of 3500–3000 cm^{-1} can be attributed to the stretching vibration and the hydrogen bond associated N–H group. Bands with maxima at about 1675 and 1450 cm^{-1} can be assigned to the asymmetric and symmetric stretching vibrations of COO^{-}, respectively. Bands at 1400 cm^{-1} assigned to O–H bond of TGA-stabilized CdTe QDs can be also observed. The formation of the hydrogen bond between $–NH_2$ of thymine and –COOH of CdTe QDs can be also postulated based on the absorption band at about 3400 cm^{-1}, on a decrease of absorption at 1680 cm^{-1} and on the presence of a broad band in the 1325–1675 cm^{-1} region [42]. One can also suggest that the splitting of C=O vibration band at 1700 cm^{-1} may result from the formation of the coordination bond between oxygen and cadmium. The presence of split bands of C–N and N–H vibrations in the range of 1500–750 cm^{-1} resulted from the hydrogen bond formation between different molecules (TGA–thymine; thymine–thymine; TGA–TGA).

3.1.2. XPS measurements. In order to gain a deeper insight into the chemical composition and the bonding state of the materials developed, XPS measurements were employed (figure 3). XPS may be applied to assess the surface compositions of the particles and it has good surface-accuracy since it only penetrates 2–10 nm deep into the sample. Thus, the atomic ratio determined employing XPS reflects the near-surface composition of the particles [43]. The sample analyzed with XPS is bombarded with x-ray photons which leads to the emission of photoelectrons from the surface whose binding energies are characteristic of the element present at the surface. The XPS spectra for CdTe QDs and CdTe–thymine conjugate are depicted in figure 3. Detected peaks are typical for Te 3d (582.6 and 572.4 eV), Cd 3d (411.9 and 405 eV), O 1 s (531.3 eV), C 1 s (285.3 eV) and S 2p (162.6 eV) [44, 45] confirming that obtained CdTe QDs are stabilized with TGA consisting of oxygen, sulfur and carbon. In the full range of XPS spectrum for CdTe–thymine conjugate the new peak of N 1 s with maximum at binding energy of 400 eV appeared and the signal from O 1 s and C 1 s became more intensive. Moreover, in the case of the conjugate the peaks assigned to Te 3d and S 2p are visible only in high-resolution XPS spectra (see inserts in figure 3). These changes might be explained considering the presence of thymine moieties bound to the QDs surface. Taking into account the fact that the XPS shows only the composition of the QD surface binding of thymine to QDs surface decreased the signals from the Cd, Te and S. Overall, the results of XPS analysis confirmed previous conclusions on CdTe QDs and CdTe–thymine composition based on elemental analysis and FTIR spectra.

3.1.3. XRD analyses. The crystalline structure of the materials was studied with the x-ray powder diffraction technique. Figure 4 shows the XRD patterns for CdTe QDs and CdTe–thymine conjugates. The XRD pattern of the CdTe QDs revealed peaks in the range of 22°–28.9°, 41.5°–44.6°

Table 2. Results of elemental analysis of CdTe QDs and CdTe–thymine conjugate.

Sample	Content (%)			
	C	H	N	S
CdTe QDs	7.27 ± 0.23	1.58 ± 0.02	—	12.95 ± 0.12
CdTe–thymine (1:6)	5.77 ± 0.01	1.23 ± 0.00	0.18 ± 0.02	6.85 ± 0.03

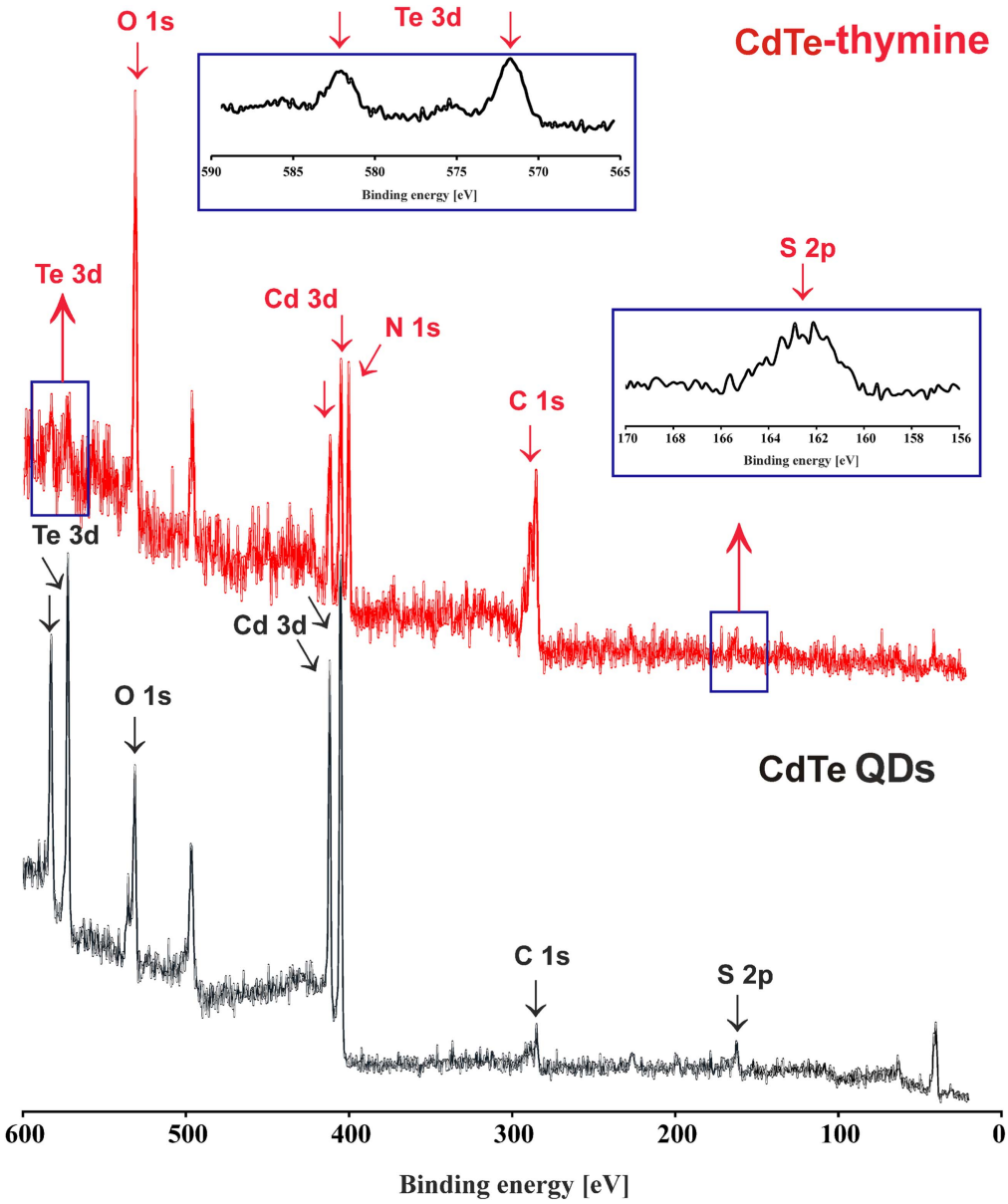

Figure 3. XPS spectra of CdTe QDs and CdTe–thymine.

and weak peak at 51.4° that could be assigned to (111), (220) and (311) diffraction planes and corresponding to cubic zinc-blende structure [46]. XRD pattern obtained for CdTe–thymine was quite similar to that for CdTe QDs, however, the new diffraction peak at 2θ of 27.5°, which might be attributed to thymine, was observed. It was previously shown that a film composed of thymine exhibits a very sharp peak at around $2\theta = 27.2°$ [47]. This peak overlaps with that for CdTe QDs and therefore might have caused its observed broadening. Additionally, we assume that the shift to higher angles in XRD pattern for CdTe–thymine conjugate may reflect the successful conjugation of nucleobase to CdTe QDs. Jiang *et al* [48] synthesized the gadolinium doped CdTe QDs and noticed that diffraction peaks of Gd:CdTe QDs were slightly shifted towards higher angles with the increase in the amount of Gd^{3+} dopant. This evidence confirms that the Gd^{3+} ions have been embedded into the crystal lattice of CdTe. Zhang *et al* [49] reported CdTe@GdS fluorescent-magnetic nanoparticles for tumor-targeted dual-modal imaging. They performed XRD analysis to show crystal structure of the CdTe QDs and the CdTe@GdS NPs. Authors have shown that the reflection peaks of the CdTe@GdS NPs shift to the higher degree region contrasting with the bulk CdTe QDs what confirmed that the GdS shell was successfully coated onto the surface of CdTe QDs. These results clearly demonstrate that the native CdTe QDs crystalline structure was retained in CdTe–thymine conjugate developed.

3.2. Determination of size and zeta potential of CdTe QDs and CdTe–thymine conjugates

The zeta potential and DLS measurements of the CdTe QDs were performed since the intensity of fluorescence and position of the plasmonic resonance band of the QDs is strongly

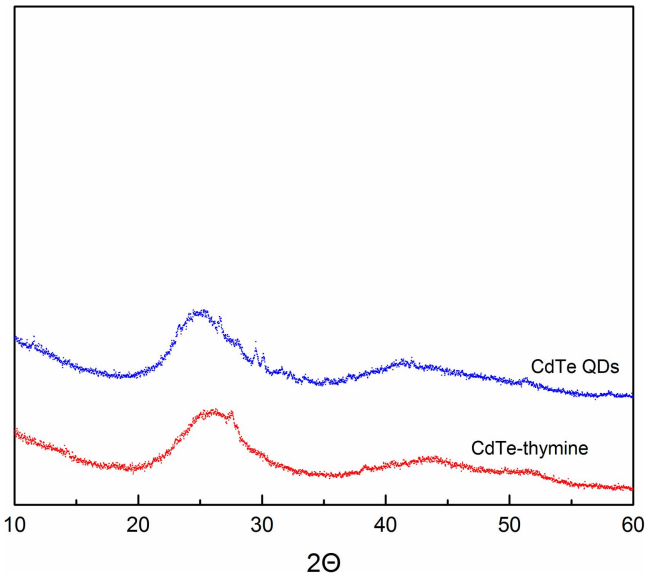

Figure 4. XRD pattern of CdTe QDs and CdTe–thymine conjugate.

dependent on their size [50]. The values of the mean hydrodynamic diameter (dz), DI and the zeta potential (ζ) found are presented in table 3. The hydrodynamic diameter of the CdTe QDs stabilized with TGA was 119.7 ± 2.2 nm whereas the size of the CdTe–thymine conjugates ranged from 196 ± 3.1 nm (for 1:1 conjugate) to 960 ± 8.7 nm (for 1:2 conjugate). Distribution profiles of the hydrodynamic diameters obtained from DLS measurements for CdTe QDs and CdTe–thymine 1:6 conjugate are presented in figure 5. As expected, the zeta potential of CdTe QDs was negative resulting from the presence of the negatively charged thiol groups at the surface of the QDs. The values of zeta potential have not changed considerably on formation of conjugates. Although the zeta potential values of all the systems indicated they can form stable aqueous dispersions, in some of them aggregates were formed as indicated by their larger size and high DI values.

Taking into account the results of both DLS and fluorescence measurements, the 1:6 conjugate was chosen as the system with the optimal properties.

3.3. Morphology of CdTe QDs and of CdTe–thymine 1:6 conjugates

The morphology of the materials obtained was studied using TEM in normal and high resolution mode (HRTEM). Figure 6 presents TEM/HRTEM micrographs of TGA-capped CdTe QDs and CdTe–thymine conjugate. One could observe that both types of materials had tendency for aggregation (figures 6(A) and (C)). The images of the aggregates clearly revealed the presence of many closely stacked nanoparticles. It was found from HRTEM images that the average size of the CdTe QDs and CdTe–thymine conjugate was 3–4 nm and 5–6 nm, respectively (figures 6(B) and (D)).

The hydrodynamic diameter obtained from DLS measurements was in the range of 120 and about 274 nm for CdTe QDs and CdTe–thymine 1:6 conjugate, respectively. The diameters of the particles found from the DLS

Table 3. The values of the mean hydrodynamic diameter (D_h), dispersity index (DI) and the zeta potential (ζ) of the conjugates studied.

Type of the material	pH	D_h (nm)	DI	ζ(mV)
CdTe QDs	7.5	119.7 ± 2.2	0.313	−37.7 ± 2.7
CdTe–thymine 1:1	7.5	196.0 ± 3.1	0.281	−38.9 ± 2.5
CdTe–thymine 1:2	7.5	960.1 ± 8.7	0.702	−36.0 ± 3.5
CdTe–thymine 1:3	7.5	458.5 ± 9.7	0.399	−34.9 ± 4.7
CdTe–thymine 1:5	7.5	776.1 ± 8.4	0.787	−36.3 ± 2.9
CdTe–thymine 1:6	7.5	273.6 ± 9.1	0.267	−37.7 ± 2.7
CdTe–thymine 1:7	7.5	308.4 ± 1.1	0.398	−39.7 ± 2.6

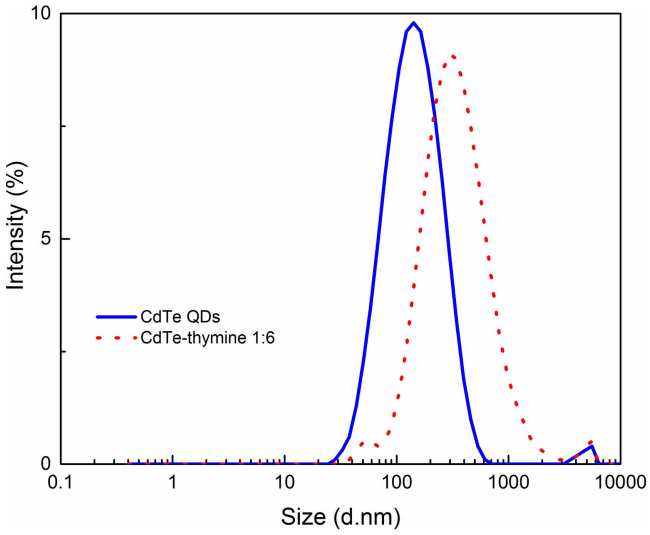

Figure 5. Distribution profiles of the hydrodynamic diameter obtained from DLS measurements for: CdTe QDs (blue line) and CdTe–thymine 1:6 conjugate (red line).

measurements were thus greater than those observed on TEM micrographs. The reason for this is that the DLS method measures the mean hydrodynamic diameter, that is the size of the particle together with the layer of ions and solvent molecules surrounding it. Additionally, since the intensity of the scattered light increases with the increasing size of the objects, the z-averaged hydrodynamic mean diameter obtained by cumulate analysis is overestimated and normally larger than that obtained by TEM [51]. The results obtained by means of these two techniques differ significantly, however, it should be emphasized that they provide the complementary information. TEM findings inform about the size and shape of the core while DLS gives a deeper insight into the particle's diameter in the aqueous medium.

To gain more insight into the morphology of the materials developed AFM studies were performed. Figures 7(A) and (B) display the AFM 3D render, while figures 7(C) and (D) present the AFM images with cross-sections of TGA-capped CdTe QDs (figure 7(C)) and CdTe–thymine conjugate (figure 7(D)), respectively. As can be seen, the CdTe QDs stabilized with TGA were reasonably well dispersed at the sample surface. The crystalline structures on their surface had the diameter equal to 2.5 ± 0.5 nm whereas the diameter of the CdTe–thymine conjugates was around 3.4 ± 0.6 nm.

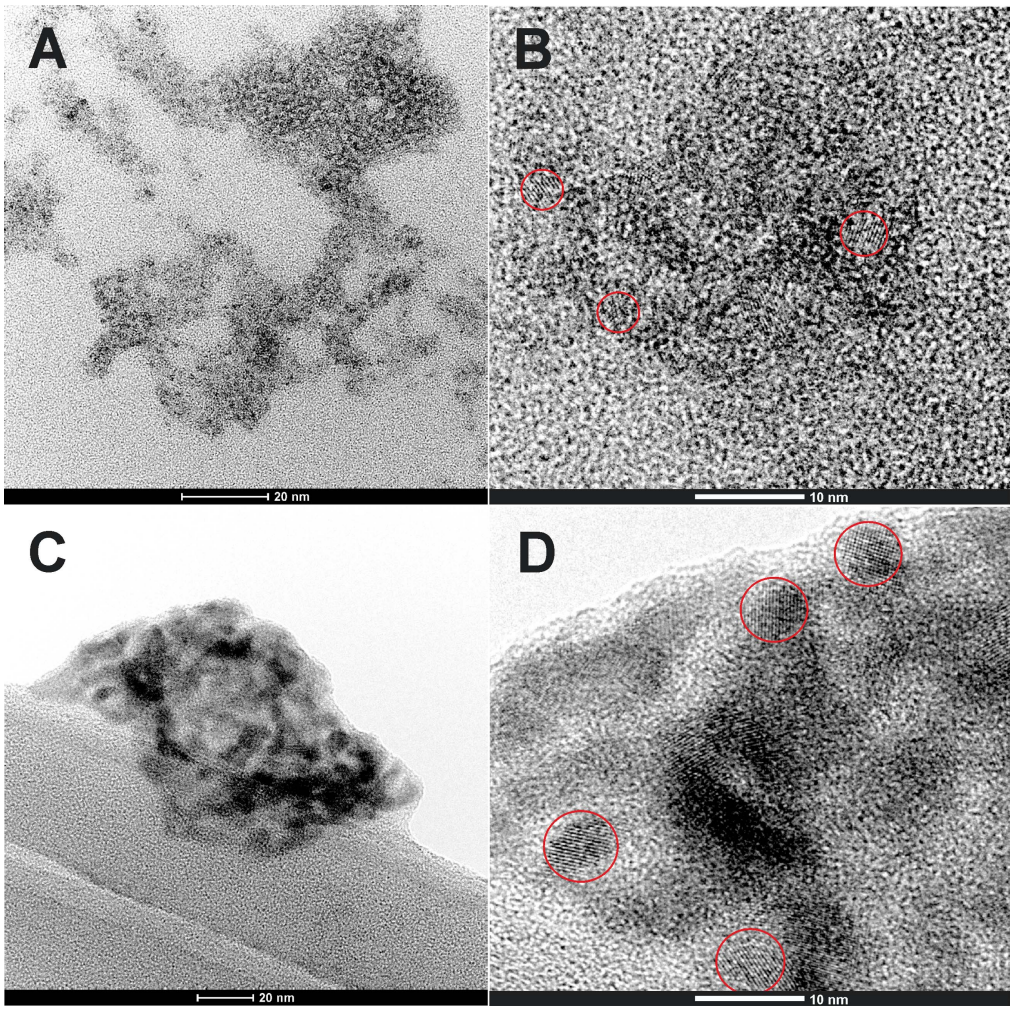

Figure 6. TEM and HRTEM micrographs of CdTe QDs: (A) (TEM), (B) (HRTEM), and of CdTe–thymine conjugates: (C) (TEM), (D) (HRTEM).

These results seem to be in accordance with the HRTEM findings. When comparing the AFM 3D render for CdTe QDs stabilized with TGA and for the CdTe–thymine conjugates some differences could also be noticed. The tendency to form aggregates is more pronounced in the case of the CdTe–thymine conjugates which might be explained considering the possible thymine-thymine interactions.

Consequently, these experiments confirmed earlier findings that thymine was successfully attached to CdTe QDs what resulted in their increased size as shown also by means of TEM/HRTEM measurements.

3.4. The UV–vis and fluorescence spectra of CdTe QDs and CdTe–thymine conjugates

The optical properties of TGA-capped CdTe QDs and CdTe–thymine conjugates were then characterized. Figure 8 shows electronic absorption and fluorescence spectra of these materials. The broad-band absorption was observed for both types of materials, typical of nanoparticles. The absorption band of the CdTe–thymine conjugate was stronger and red shifted with respect to that of the CdTe QDs. These differences can be explained considering the interaction between Cd^{2+} ions present at the surface of CdTe QDs and the oxygen atoms of thymine [41], as well as with the differences in the size of these nanoparticles. The fluorescence spectra displayed the plasmonic resonance emission band at about 540 nm on excitation at 351 nm. The emission spectra of both CdTe QDs and CdTe–thymine conjugate were characterized by a symmetric band. The full-width at half-maximum (FWHM) of fluorescence emission band for CdTe QDs was 46 nm and for CdTe–thymine conjugate 37 nm. That may suggest that the optical properties of CdTe–thymine conjugate was superior over the pristine CdTe QDs. According to the literature, narrow and visible luminescence peaks are observed with FWHM value in the range of 38–52 nm [33]. Other researchers [52] reported that PL spectrum of CdTe QDs and CdTe-adenine was characterized by good symmetry and was sufficiently narrow with FWHM of 66 nm and 49 nm, respectively.

Interestingly a red shift in the absorption spectra of obtained conjugate was observed while no noticeable shift in the emission spectra was seen. This phenomenon might be explained considering the Stokes shift which is commonly observed in semiconductor QDs. In order to explain the origin

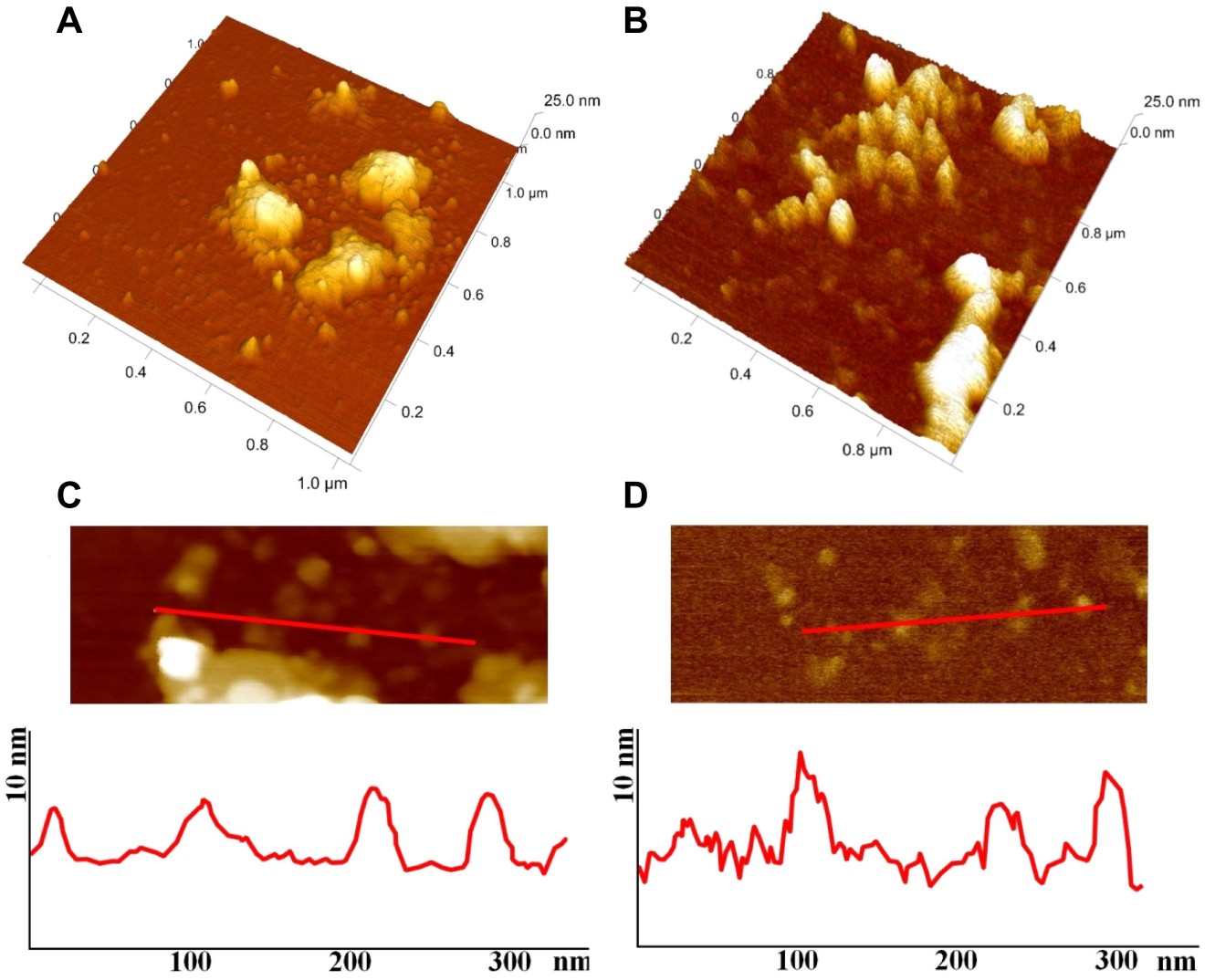

Figure 7. AFM 3D render for CdTe QDs (A), CdTe–thymine conjugate (B) and AFM images with cross-sections for CdTe QDs (C) and CdTe–thymine conjugate (D).

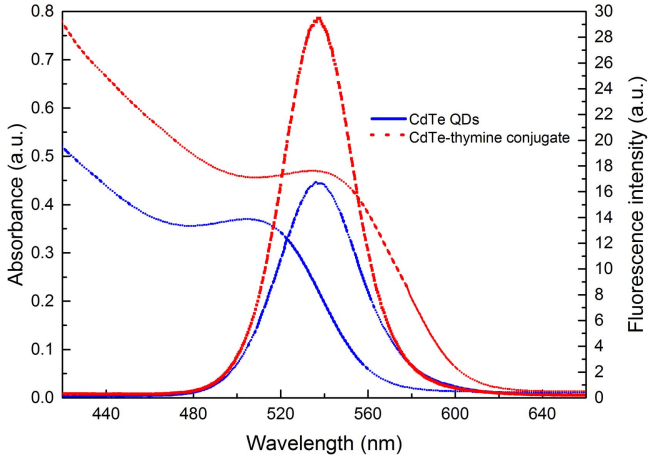

Figure 8. UV–vis absorption and fluorescence spectra of CdTe QDs and CdTe–thymine conjugate (the concentration of CdTe QDs was 0.125 mg ml^{-1}).

of the Stokes shift in QDs two different mechanisms were proposed. The process of absorption occurs with participation of chemical moieties being in the ground S electronic state which lies deeper than an optically passive state (P state) in the valence band to form an exciton in the singlet state of the electron and hole. The first mechanism postulated that the deexcitation takes place into the P state with the help of phonons and therefore the Stokes shift is given by ΔE_{SP} (the difference in energy between the exciton states formed with S and P hole states) [53]. According to the second mechanism [54] the exciton in the singlet state first thermalizes into a triplet from where it deexcites with the help of phonons either to the S state, with the Stokes shift given by ΔE_{ST} (representing the singlet-triplet splitting) or to the P state at the top of the valence band, with the Stokes shift: $\Delta E_{SP} + \Delta E_{ST}$. In addition to these mechanisms, the redshift might be also observed if the initial ground state and the final excited state

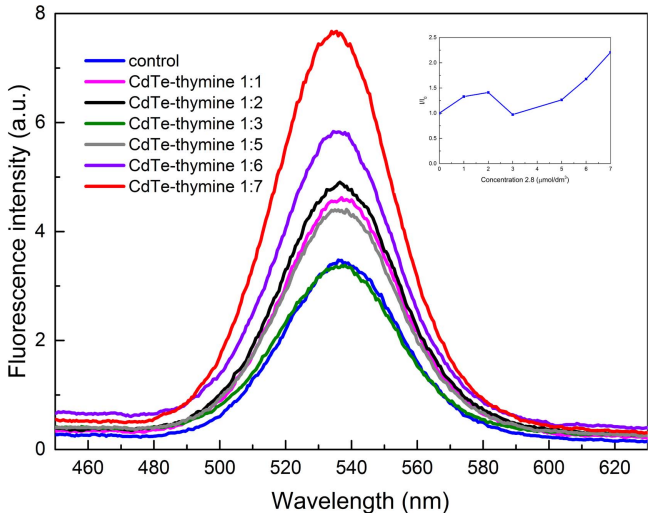

Figure 9. The fluorescence emission spectra of CdTe–thymine conjugates obtained using different CdTe:thymine molar ratio, $\lambda_{exc} = 351$ nm. (Insert: dependence of the relative fluorescence intensity (I/I_0) on the CdTe:thymine molar ratio used during their synthesis.)

have a different atomic configuration. Such a red shift, known as Frank–Condon shift, is commonly observed in molecules and it points to the defects in solids and may be also relevant in ultrasmall QD's [55].

According to the literature, Stokes shift decreases with an increase in the radius of the dot and disappears beyond a certain radius [56]. Moreover, Fei *et al* in their study on the CdTe/CdS core–shell structured QDs demonstrated that the Stokes shift decreases with increasing core–shell ratio, which can be ascribed to the strength of the electron–phonon coupling increasing with the core–shell ratio of the nanocrystal increasing [57]. Considering the literature findings it might be postulated that thymine conjugation strongly affected the electronic state of CdTe-QDs inducing the red shift in absorbance spectra and thus reducing Stokes shift.

The position of the fluorescence band was not dependent on the amount of thymine in the CdTe–thymine conjugate but the intensity of the emission band was influenced by that parameter (see figure 9). The fluorescence intensity of CdTe–thymine conjugates was generally growing with an increase in thymine concentration, although not monotonically. The highest fluorescence intensity was observed when the molar ratio of CdTe to thymine in the reaction mixture was 1:7 (see table 1). That can be explained considering the coordinated interactions between the surface of CdTe QDs and the nitrogen atoms of thymine as well as with the hydrogen bond formation. These interactions can effectively remove the dangling bonds and surface defects, resulting in higher fluorescence intensity of CdTe–thymine conjugates [52]. It was also suggested that by removing of local energy traps on surface and by neutralizing of the surface charge one may increase the PL intensity [41]. There is, however, a limit to which the surface of QD can be modified with thymine, because too high content of biomolecules introduced can destabilize this colloidal system resulting in the QDs aggregation and reduced fluorescence intensity.

3.5. Interaction of CdTe–thymine conjugates with nucleobases and modified nucleosides studied with fluorescence spectroscopy

Finally, the interaction of CdTe–thymine conjugates with adenine, the nucleobase complementary to thymine, was studied. CdTe–thymine conjugate (1:6, pH = 7.5) was titrated with adenine and, to determine the selectivity of the conjugate-adenine interaction, also with other nucleobases. It was observed that fluorescence intensity of CdTe–thymine conjugate increased considerably on addition of adenine and this effect is especially pronounced for adenine concentration up to 0.7 mmol ml^{-1} (see figure 10(B)). This effect could not be ascribed to dilution as shown in a separate experiment. For higher concentrations of the titrant the fluorescence intensity reached a plateau and then decreased slightly (10 A). For other nucleobases the effect of fluorescence enhancement with growing nucleobase concentration was much smaller (figure 10).

The experiment has proven high sensitivity and selectivity of CdTe–thymine conjugate fluorescence towards adenine. This may be attributed to the specific interactions between thymine and adenine, as reported in the literature [58]. Figure 11 demonstrates the proposed mechanism of CdTe–thymine conjugate interaction with adenine.

Furthermore, to evaluate the applicability of the obtained materials for detection of modified nucleosides in body fluids, the interaction of CdTe–thymine conjugates with 5′-deoxy-5′-(methylthio)adenosine (MTA) and 2′-O-methyladenosine was also evaluated in a similar way as for nucleobases. As shown in figure 12, the fluorescence intensity of CdTe–thymine conjugate is significantly enhanced in the presence of MTA and 2′-O-methyladenosine. This effect could not be ascribed to dilution as shown in a separate experiment

Figure 13 demonstrates the proposed mechanism of CdTe–thymine conjugate interaction with both types of modified nucleosides.

The modified adenine-containing nucleosides studied have been chosen because they have been identified as the urinary tumor markers and hence finding a method of their detection and quantitation may provide a way of cancer diagnosis and progression. Moreover, urinary nucleosides may also indicate the occurrence of other diseases such as AIDS, cystic fibrosis and severe immunodeficiency disease resulting from the deficiency of adenosine deaminase (ADA). Moreover, it is known that the accumulation of 2′-O-methyladenosine could play a role in the pathological processes in ADA-deficient patients [59]. Moreover, MTA can be also found in human urine. That compound is a substrate of 5′-methylthioadenosinephosphorylase (MTAP), an enzyme known to be expressed by tumor suppressor genes [60].

Based on these preliminary experiments one can postulate that the CdTe–thymine conjugate we developed can serve as a working component for the selective biosensor of adenine and/or its compounds.

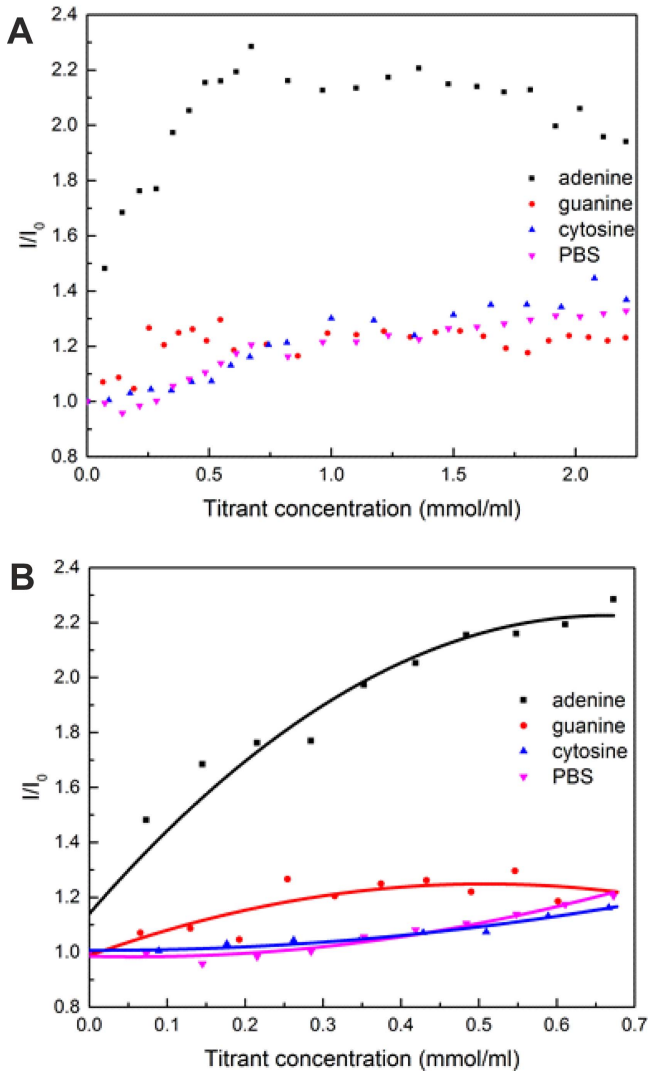

Figure 10. Dependence of the relative fluorescence intensity (I/I_0) of CdTe–thymine conjugates in the presence of nucleobases: adenine, guanine and cytosine (pH = 7.5, λ_{exc} = 351 nm) for the long (A) and (B) the short range of the titrant concentration To show the effect of dilution, fluorescence was also measured upon the addition of corresponding volumes of PBS solution.

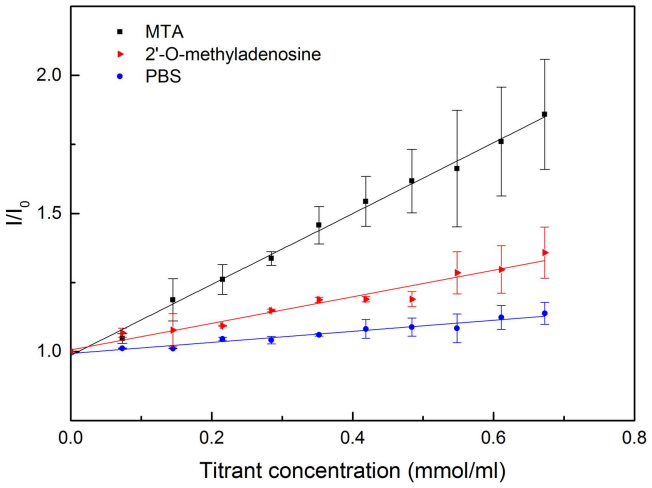

Figure 12. Dependence of the relative fluorescence intensity (I/I_0) of CdTe–thymine conjugates in the presence of MTA and 2′-O-methyladenosine. To show the effect of dilution, fluorescence was also measured upon the addition of corresponding volumes of PBS solution.

4. Conclusions

Novel fluorescent material based on TGA-capped CdTe–thymine conjugates has been developed and thoroughly characterized. CdTe QDs stabilized with TGA forming stable aqueous dispersion with excellent fluorescence properties were synthesized. Successful conjugation of TGA-protected CdTe QDs with thymine was confirmed by elemental analysis, FTIR, DLS, TEM/HRTEM and AFM measurements. Crystal structure and composition of the CdTe QDs and their conjugates with thymine were characterized by means of XRD and XPS techniques. It was demonstrated that the size of conjugates was 4–6 nm and that the native CdTe QDs crystallization was retained in CdTe–thymine conjugate developed. It was shown that coordination and hydrogen bonds between thymine and CdTe QDs enhanced fluorescence intensity and increased the stability of the CdTe QDs. The conjugate with the optimal composition (QDs/thymine

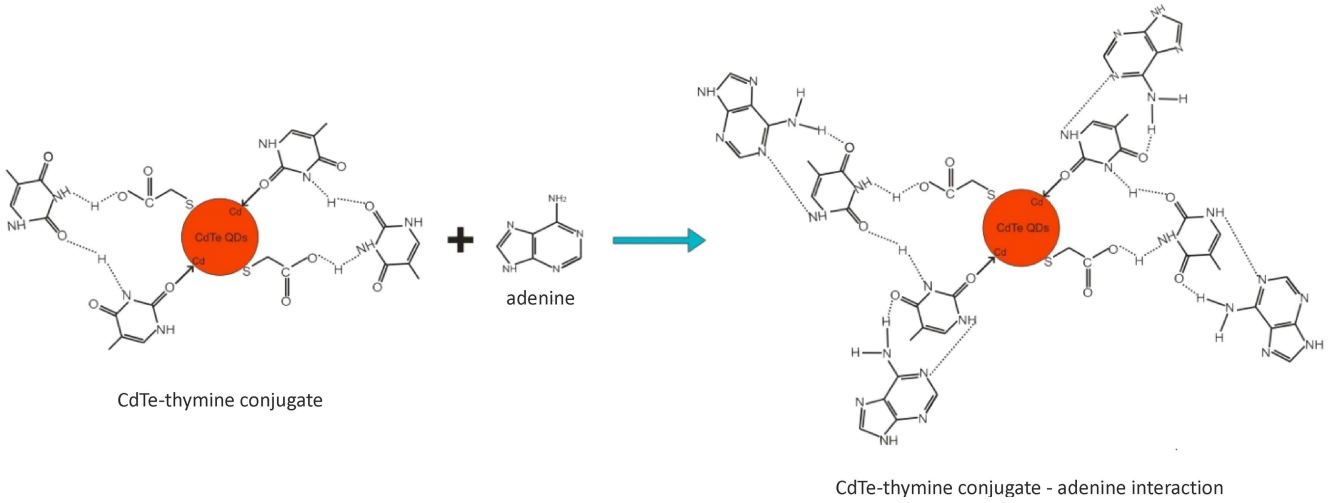

Figure 11. The mechanism of interaction between CdTe–thymine conjugate and adenine.

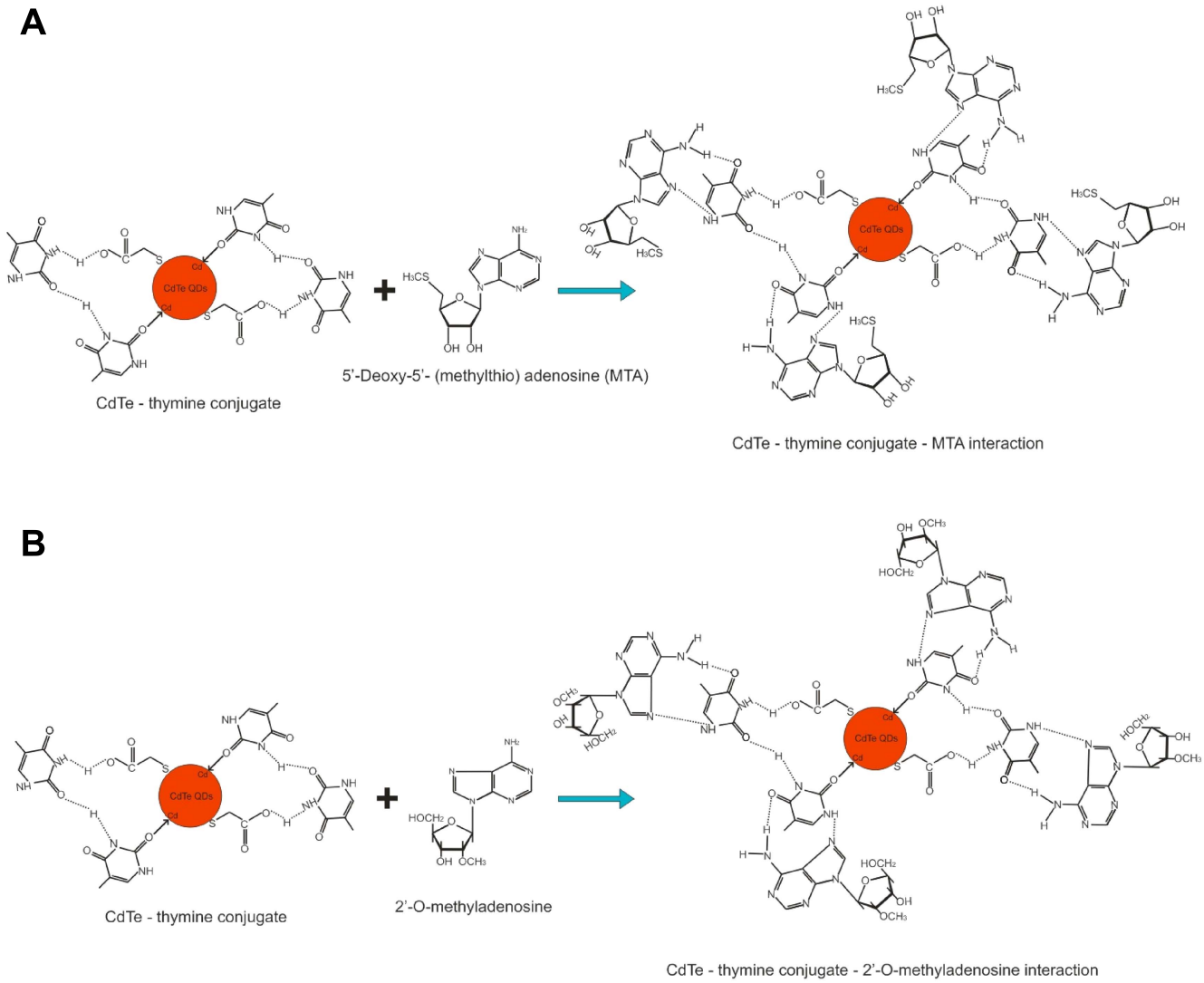

Figure 13. The proposed mechanism of interaction between CdTe–thymine conjugate and modified adenosines, (A) 5′-deoxy-5′-(methylthio) adenosine (MTA), B 2′-O-methyladenosine.

of 1:6 mol mol^{-1} in the reaction mixture) interacted strongly with adenine and with modified nucleosides, 5′-deoxy-5′-(methylthio)adenosine and 2'-O-methyladenosine, which are known as cancer biomarkers. High sensitivity and selectivity of CdTe–thymine fluorescence towards adenine and modified adenosine suggests that it can be potentially useful for development of the biosensor for adenine/adenosine biomarkers.

Acknowledgments

The project was financed by Polish National Science Centre grant UMO-011/03/B/ST5/01559 and by the grant from Foundation for Polish Science Team Programme cofinanced by the EU European Regional Development Fund, PolyMed, TEAM/2008-2/6. ŁR acknowledges the financial support of National Science Centre, Poland, grant 2016/21/N/ST5/00883.

References

[1] Cui L, He X P and Chen G R 2015 *RSC Adv.* **5** 26644
[2] Ma Y, Li Y, Ma S and Zhong X 2014 *J. Mater. Chem.* B **2** 5043–51
[3] Kim K, Jeong S, Woo J Y and Han C-S 2012 *Nanotechnology* **23** 065602
[4] Du J, Wu Y, Hao X and Zhao X 2011 *J. Mol. Struct.* **1006** 650–4
[5] Sun H, Zhang F, Wei H and Yang B 2013 *J. Mater. Chem.* B **1** 6485–94
[6] Fan J-W, Vankayala R, Chang C-L, Chang C-H, Chiang C-S and Hwang K C 2015 *Nanotechnology* **26** 215703
[7] Shen Y, Liu S, Yang J, Wang L, Tan X and He Y 2014 *Sensors Actuators* B **199** 389–97
[8] Xie X, Ma D and Zhang L-M 2015 *RSC Adv.* **5** 58746–54
[9] Lira R B, Seabra M A B L, Matos A L L, Vasconcelos J V, Bezerra D P, de Paula E, Santos B S and Fontes A 2013 *J. Mater. Chem.* B **1** 4297–305
[10] Ensafi A A, Kazemifard N and Rezaei B 2015 *RSC Adv.* **5** 40088–93

[11] Wang Y, Hu R, Lin G, Law W-C and Yong K-T 2013 *RSC Adv.* **3** 8899–908
[12] Vannoy C H, Chong L, Le C and Krull U J 2013 *Anal. Chim. Acta* **759** 92–9
[13] Liu S, Shi F, Chen L and Su X 2013 *Talanta* **116** 870–5
[14] Frasco M F and Chaniotakis N 2009 *Sensors* **9** 7266–86
[15] Huang S, Xiao Q, Li R, Guan H-L, Liu J, Liu X–R, He Z-K and Liu Y 2009 *Anal. Chim. Acta* **645** 73–8
[16] Chen Z, Ren X, Meng X, Zhang Y, Chen D and Tang F 2012 *Anal. Chem.* **84** 4077–82
[17] Algarra M, Campos B B, Alonso B, Miranda M S, Martínez Á M, Casado C M and Esteves da Silva J C G 2012 *Talanta* **88** 403–7
[18] Yan Y, Wang S, Liu Z, Wang H and Huang D 2010 *Anal. Chem.* **82** 9775–81
[19] Zhang F 2016 *Near-infrared Nanomaterials: Preparation, Bioimaging and Therapy Applications* (Cambridge: RSC Publishing)
[20] Borisov S M and Wolfbeis O S 2008 *Chem. Rev.* **108** 423–61
[21] Chao J, Zhu D, Zhang Y, Wang L and Fan C 2016 *Biosens. Bioelectron.* **76** 68–79
[22] Ebrahim S, Reda M, Hussien A and Zayed D 2015 *Spectrochim. Acta* A **150** 212–9
[23] Wang L, Song J, Liu S, Hao C, Kuang N and He Y 2015 *J. Colloid Interf. Sci.* **457** 162–8
[24] Liu Z, Liu S, Wang X, Li P and He Y 2013 *Sensors Actuators* B **176** 1147–53
[25] Li L, Lu Y, Ding Y, Zhang F and Wang Y 2012 *Can. J. Chem.* **90** 173–9
[26] Monajjemia M and Chahkandi B 2005 *J. Mol. Struct.* **714** 43–60
[27] Mallajosyula S S, Datta A and Patim S 2005 *Synth. Met.* **155** 398–401
[28] Ren S, Wang H, Zhang H, Yu L, Li M and Li M 2015 *J. Electroanal. Chem.* **750** 65–73
[29] Tedsana W, Tuntulani T and Ngeontae W 2013 *Anal. Chim. Acta* **783** 65–73
[30] Wang C, Hu Z, Xu S, Zhou S, Wang Z and Cui Y 2015 *Nanotechnology* **26** 125703
[31] Yuwen L, Bao B, Liu G, Tian J, Lu H, Luo Z, Zhu X, Boey F, Zhang H and Wang L 2011 *Small* **7** 1456–63
[32] Fan H, Chen Z, Blinker C J, Clawson J and Alam T J 2005 *Am. Chem. Soc.* **127** 13746–7
[33] Gaponik N, Talapin D V, Rogach A L, Hoppe K, Shevchenko E V, Kornowski A, Eychmüller A and Weller H J 2002 *Phys. Chem.* B **106** 7177–85
[34] Owens S A, Carpenter M C, Sonne J W H, Miller C A, Renehan J R, Odonkor C A, Henry E M and Miles D T 2011 *J. Phys. Chem.* C **115** 18952–7
[35] Wang J, Han S, Ke D and Wang R 2012 *J. Nanomaterials* **2012** 1–8
[36] Zhang H, Zhou Z, Yang B and Gao M 2003 *J. Phys. Chem.* B **107** 8–13
[37] Wei X, Zhou Z, Hao T, Li H, Dai J, Gao L, Zheng X, Wang J and Yan Y 2015 *J. Lumin.* **161** 47–53
[38] Jhonsi M A and Renganathan R 2010 *J. Colloid Interf. Sci.* **344** 596–602
[39] Zhang Y, Mi L, Wang P-N, Mab J and Chen J-Y 2008 *J. Lumin.* **128** 1948–51
[40] Abd El-sadek M S and Babu S M 2010 *Physica* B **405** 3279–83
[41] Feng X, Shang Q, Liu H, Wang W, Wang Z and Liu J 2010 *J. Lumin.* **130** 648–53
[42] Singh J S 2008 *J. Mol. Struct.* **876** 127–33
[43] Han Z, Wang L, Zhu J, Zhang S and Zhou W 2011 *J. Appl. Polym. Sci.* **122** 43–9
[44] Li Z, Xu W, Wang Y, Shah B R, Zhang C, Chen Y, Li Y and Li B 2015 *Carbohydr. Polym.* **121** 477–85
[45] Khatei J and Koteswara Rao K S R 2011 *Mater. Chem. Phys.* **130** 159–64
[46] Huang Y, Liu J, Yu Y and Zuo S 2015 *J. Alloys Compd.* **647** 578–84
[47] Silaghi S M Optical characterisation of DNA bases on silicon surfaces *PhD Thesis* Technische Universität Chemnitz
[48] Jiang C, Shen Z, Luo C, Lin H, Huang R, Wang Y and Peng H 2016 *Talanta* **155** 14–20
[49] Zhang F, Kong X-Q, Li Q, Sun T-T, Chai C, Shen W, Hong Z-Y, He X-W, Li W-Y and Zhang Y-K 2016 *Talanta* **148** 108–15
[50] Qu L and Peng X 2002 *J. Am. Chem. Soc.* **124** 2049–55
[51] Kępczyński M, Bednar J, Lewandowska J, Staszewska M and Nowakowska M 2009 *J. Nanosci. Nanotechnol.* **9** 3138–43
[52] Feng X, Shang Q, Liu H, Wang H, Wang W and Wang Z 2009 *J. Phys. Chem.* C **113** 6929–35
[53] Li J and Xia J B 2000 *Phys. Rev.* B **61** 15880
[54] Efros A L, Rosen M, Kuno M, Nirmal M, Norris D J and Bawendi M G 1996 *Phys. Rev.* B **54** 4843
[55] Franceschetti A and Pantelides S T 2003 *Phys. Rev.* B **68** 033313
[56] Bagga A, Chattopadhyay P K and Ghosh S 2006 *Phys. Rev.* B **74** 035341
[57] Fei X, Jia G and Wang J 2010 *Chalcogenide Leters* **7** 83–7
[58] Di G 2016 *Biophys. Chem.* **208** 76–83
[59] Mikulska A, Inoue M, Kuroda K, Iwanowska A, Yusa S-I, Nowakowska M and Szczubiałka K 2014 *Eur. Polym. J.* **59** 230–8
[60] Andreu-Pérez P, Hernandez-Losa J, Moliné T, Gil R, Grueso J, Pujol A, Cortés J, A Avila M and Recio J A 2010 *BMC Cancer* **10** 265